Status Report No. 6

NOISE INVESTIGATIONS WITH IMPINGING JET FLOWS

by

Darshan S. Dosanjh

and

Francis J. Montegani

Submitted to

National Aeronautics and Space Administration

Grant No. NsG-431

SYRACUSE UNIVERSITY RESEARCH INSTITUTE

Department of Mechanical & Aerospace Engineering

Report No. ME-1085-660606

June 1966

Summary

Further investigations of the far field noise radiation from an underexpanded convergent axisymmetric (D = 3/8 in.) main jet flow which is impinged in its first shock cell by a concentric annular (3/4 in. diam. x 3/64 in. wide) jet flow were conducted in an anechoic chamber. The main jet flow was normally operated at a total pressure of 100 psig. The impinging annular flow was directed either normal to, or at 45° to, the main jet axis. The impingement location in the first shock cell was also varied. Percent impingement (defined as $100 \frac{\text{impinging jet total gage pressure}}{\text{main jet total gage pressure}}$) was varied from 0 - 50%. Experimental data for the far field noise radiation from both the main jet flow alone and the interacting jet flows were recorded yielding the total acoustic power radiated, directional patterns, and 1/3 octave band power spectra. At low values of percent impingement, the total acoustic power radiated increased from about 142 dB re 10^{-13} watt at zero percent control to 148 dB at 8% impingement. Between 8 and 33% impingement, the power radiated then decreased to a relative minimum (about 144 dB) that occurred between 15 and 25% impingement depending on the location of the impinging flow in the first shock cell. At still higher values of percent impingement the power radiated increased again. The corresponding flow characteristics at different values of percent impingement were optically recorded revealing acoustic sources and marked changes in the shock structure of the interacted jet flow. A possible relationship between the total acoustic power

radiated and the observed acoustic sources and the changes in the shock geometry and flow structure is examined and explanations are advanced accounting for some of the interesting features of the observed power radiation behavior.

Introduction

This semiannual status report includes the results of Noise Investigation with Impinging Jet Flows conducted at Syracuse University under NASA Grant No. NsG-431, during the period from December 1, 1965 to May 31, 1966. The experimental facilities with which this research on noise from interacting high speed jet flows was conducted and the methods of measurement and computation are fully described in Refs. 1, 2, 3, and 4 and therefore are only briefly mentioned here. All acoustical data were obtained in an anechoic chamber. The microphone was positioned successively at 8 far field measuring stations spaced at 15° increments of azimuth angle starting from the downstream jet axis in a horizontal plane midway between the ceiling and floor wedge tips which were 9 feet apart. A schematic plan of the arrangement is given in Fig. 1. At each measuring station, either overall sound pressure level data or 1/3 octave band spectrum data, and occasionally both, were obtained. From these data, total acoustic power radiated and 1/3 octave band power spectra were computed by numerical integration using a digital computer. Sound pressure level measurements could be repeated for any operating conditions within 0.5 dB. At each measuring station, the measured overall sound pressure level agreed within 1.0 dB with that computed from the 1/3 octave band power spectrum.

Shadowgraphs of the jet flows were also taken in the anechoic chamber using portable remotely operated optical equipment which was removed from the chamber during acoustical measurements. These shadowgraphs permitted determination of the flow behavior including geometry

of the shock structure and the identification of strong acoustic sources in the flow. These observations were tentatively used to account for the nature and the behavior of the observed sound radiation and are discussed in this report.

Nozzle Geometries

The nozzle arrangement used in these investigations are shown in Fig. 2. Three configurations of the basic nozzle arrengement were investigated:

a) The main jet alone, with no impinging jet nozzles in place;

b) the main jet interacting with an annular jet impinging at 90°; and

c) the main jet interacting with an annular jet impinging at 45°.

For the interacting jet flow experiments, percent impingement which is defined as the ratio, as a percent, of the impinging jet total gage pressure p_{ti}, to the main jet total gage pressure p_t, was varied from zero to 50%. The downstream location of the impinging jet nozzle exit was also varied. This location is given by the non-dimensional ratio x/D, where x is the distance from the plane of the main jet exit to the plane of the centroid of the annular jet generatrix, and D is the main jet exit diameter. The x/D ratio was varied from 0.10 to 1.0. The main jet exit diameter was 3/8 in. for these investigations, and the annular impinging jet nozzles were of equal exit area as the main jet, and were 2D in diameter x D/8 wide (or 3/4 in. in diameter x 3/64 in wide). The main jet was normally operated at a reservoir pressure of 100 psig.

Noise and Optical Studies with Main Jet Alone

For the main jet alone and with the impinging jet nozzle removed, directivity, power level, and power spectrum were determined as functions of jet operating pressure p_t. These data established a basis for comparison with similar data for the interacting jet flows.

The acoustic power radiated by the main jet as a function of jet pressure is given in Fig. 3a, and is linear over a wide range of pressure. The linear power level increase starts at approximately 60 psig which corresponds to the condition reported by Lassiter and Hubbard (Ref. 5) where the screech attributable to the resonance phenomenon described by Powell (Ref. 6) ceases.

The overall directivity data as measured are given in Fig. 3b showing the maximum sound pressure level occurring at 30°.

The 1/3 octave band power spectrum for the main jet alone at 100 psig with the impinging jet nozzle removed is given in Fig. 3c. The spectrum displays no discrete components.

A typical computer printout of the 1/3 octave band sound pressure levels re 2×10^{-4} μbar is reproduced in Fig. 4 in which the directivity variation with frequency may be noted. The computer takes in the observed 1/3 octave band instrument readings for each of the 8 measuring stations, corrects them for instrument setting and microphone response, and prints the correct sound pressure levels as shown in Fig. 4. At each station the overall sound pressure level is computed from the 1/3 octave band data and is printed below the spectrum analysis. From the overall sound pressure levels, the total acoustic power radiated is computed and printed last, both in dB re 10^{-13} watt and watts.

Under certain operating conditions the shock system observed in the interacting flows were very similar to those of an underexpanded single convergent axisymmetric jet. Therefore shadowgraphs of the main jet alone from 10 to 100 psig were taken to establish a basis for comparison of the flow and shock structure with those of the interacting jets. The shadowgraphs for the single jet are not presented here since such jet flow behavior is well known. Some shock geometry data for the single jet is given in Fig. 10b.

Main Jet with 90° Impingement: Noise Studies

The total acoustic power radiated by the interacting jets with 90° impingement is given in Fig. 5 as a function of percent impingement for a range of x/D values. For x/D values between approximately 0.2 and 0.8, the power radiated demonstrated an interesting, repeatable and well defined behavior. For discussion purposes, consider the power level variation with percent impingement at x/D = 0.604. From 0 to 8% impingement the power level increased. At 8% it peaked 5 dB above the starting level and then decreased with increasing impingement to a relative minimum occurring at 18% impingement 1 dB above the starting level. The value of percent impingement at which the relative minimum power level occurred increased with decreasing x/D. The power level then increased again to values at the highest impingement which were one dB or so greater than that of the previous maxima. The jump in power level between 35 and 40 percent impingement clearly occurred as shown in all the experiments and was attributed to actual flow phenomena and not to data scatter.

The sound pressure levels as functions of aximuth angle are reproduced in Figs. 6a,b,c, in which the change in directional pattern of the broadband noise with percent impingement is evident. The impinging flow has little effect on the peak radiation in the 30° direction which is clearly evident at all conditions. Up to 38 percent impingement, a second peak appears at 90° with varying magnitude, but always weaker than the peak at 30°. Beyond 38 percent impingement another peak occurs at 60° also varying in magnitude which at 42 percent exceeds slightly that occurring at 30°.

Spectrum analysis of the sound radiated by the interacting jet was carried out for the case of 90° impinging flow at x/D = 0.600. Typical 1/3 octave band power spectra are presented in Fig. 7. All the spectra, with the exception of those for which the relative minimum power level occurred, displayed a discrete component in the 6300 or 8000 cps center frequency band. Such a peak did not appear in the data for the main jet alone with the impinging jet nozzle removed, although it did appear for conditions with no impinging flow but with the impinging jet nozzle in place. Consequently, the peak in the spectrum was attributed to the geometry of the nozzle arrangement and not to the flow interaction. Carefully sealing the impinging jet nozzle with lead, but otherwise not altering the exit cavity formed by the annular jet nozzle, served only to diminish the peak in the spectrum but not to eliminate it. Thus the discrete signal is not due solely to the cavity formed by the exterior surfaces of the impinging jet nozzle but must in some way also be partly due to a resonance phenomena in the cavity upstream of the impinging jet nozzle exit. The absence of this discrete component for interacting flow

conditions when the relative minimum radiated power level occurred will be examined further when more data are accumulated.

To establish the influence of the geometry-attributable discrete signal on the previously discussed power level variation with percent impingement, power levels were computed from 1/3 octave band spectral data discounting the power contribution attributable to the peak whenever it occurred. The results are presented in Fig. 8. The upper curve is the power level computed from spectrum data without modification and reproduces the results presented in Fig. 5 for x/D = 0.600. The lower curve was computed from the same data from which the peak was eliminated, that is, a smooth spectrum was assumed. Though slightly attenuated, the lower curve still demonstrates the previously described power level variation with percent impingement and therefore the observed behavior is attributable to changes in the flow the associated acoustic sources and shock structure of the combined interacted jet flows.

To examine further the role of the cavity another arrangement of the main and impinging jet nozzles have been designed and machined. It preserves the nozzle exit geometry of the jets discussed here (Fig. 2), but somewhat modifies the cavity and permits free entrainment of air into the interacting jet flow between the main jet and the annular jet where entrainment is not possible in the present arrangement (see Fig. 2). The noise radiating properties of the interacting flows from the new nozzle arrangement will be investigated in the near future and compared with the studies reported here. At the present time an investigation of the nature of the interacting flow from the new nozzles is underway. Both

optical (including shadow, schlieren, and interferometric) and pressure recording techniques are being used. Since the main purpose of this related investigation is to gather data about the actual behavior of the interacting jet flows in or around the first shock cell and not the far field acoustic measurements, the experiments are being conducted in an ordinary laboratory environment (i.e. not in an anechoic chamber) using an available independent jet flow control system. This will permit simultaneous uninterrupted progress on the noise measurements in the anechoic chamber.

Main Jet with 90° Impingement: Shadowgraphic Studies

Using the nozzle arrangement in Fig. 2, shadowgraphs of the main jet alone and also its interaction with the impinging jet at 90° were taken at operating conditions identical to those of the previously discussed acoustical results. Typical shadowgraphs are reproduced in Fig. 9 showing the development of the flow and shock structure with percent impingement at x/D = 0.600.

At zero percent impingement and with the impinging jet nozzles in place, the distance from the main jet nozzle exit to the normal shock disc and the normal shock diameter were the same as for a free convergent axisymmetric jet operating at 100 psig. These shocks geometry measurements agreed closely with those of Love, et al., Ref. 7.

With the addition of impinging flow, the intercepting shocks moved inward and the diameter of the normal shock decreased. The cell length became smaller and the reflected shocks grew in length (see Fig. 10). As this development of shock structure occurred the total acoustic power radiated increased rapidly (Fig. 5). The normal shock disc did not

disappear completely but reached a minimum diameter of 0.12D where D is the main jet diameter (3/8"). At this point in the sequence as percent impingement increased, new oblique shock structure was created tangent to and downstream of the original reflected shocks (Fig. 9b). The emergence of this new shock structure coincided approximately with the peak acoustic radiation from the interacting jet flow. For impingement of the annular jet at x/D = 0.400 and 0.800 at which the values of percent impingement corresponding to the peak power radiation were slightly different, the shock structure, based on preliminary shadowgraphic data at these two conditions, appeared to be identical. That is, for the values of x/D between 0.4 and 0.8, the peak power radiation appeared to be associated with the emergence of the new oblique shock structure regardless of the value of percent impingement at which the peak power radiation occurred. The new shock structure moved downstream with increasing percent impingement and a regular repetitive pattern of oblique shock waves was established (Fig. 9d). The establishment of this regular shock pattern spanned the percent impingement range where the total acoustic power radiated achieved the relative minimum discussed earlier. The occurrence of this relative minimum for annular jet impingement at x/D = 0.400 and 0.800 took place at significantly different values of percent impingement. Preliminary shadowgraphic data at these conditions indicated that for all x/D values, the relative minimum power radiation occurred at percent impingement conditions where the shock structure in the interacted jet flow in all cases was identical and exhibited the repetitive pattern indicated above (see Fig. 9d). At these conditions weak annular eddies were evident at the

nozzle exit, and with further increase in percent impingement, these eddies grew in prominence and a discrete 28 kcps sound signal appeared also. These are clearly evident in Fig. 9f and characterized the flow behavior up to 50 percent impingement, the highest percent impingement value investigated (Fig. 12f). As additional experimental data are accumulated and examined the interrelationship between the nature of the acoustic radiation and the flow and shock structure is expected to become more definitive.

Some recent experimental and analytical studies by the first author with interacting two-dimensional high speed jet flows indicate that due to the proximity of the impinging flow to the exit of the main jet, the effective exit pressure of the main jet is modified. That is, the impinging flow serves to modify the effective exit boundary conditions of the main jet by increasing the main jet exit pressure and it results in the interacting jet flow effectively operating at a lower pressure ratio than the single main jet.

The initial behavior of the intercepting shocks and the normal shock disc with increasing percent impingement qualitatively support this possibility since cell length and normal shock extent are diminishing, which behavior characterizes a jet operating at diminishing pressure ratios (see Ref. 7). The repetitive shock pattern and the discrete radiation occurring at higher percent impingements are characteristic of jets operating at still lower pressure ratios. A comparison of cell length and normal shock disc diameter for the 90° interacting jets at $x/D = 0.600$ with those of the main jet alone is made in Fig. 10. There is no unique correspondence of operating conditions of the main jet flow

alone and the interacting jets flow based on these two shock geometry measurements simultaneously since if cell lengths are equal in both flows for certain operating conditions, disc diameters are not equal, and vice versa. Cell lengths and disc diameters in the two flows are equal simultaneously only for the main jet at 52 psig and the interacting jets at 21 percent impingement, approximately. These observations will be examined further after more experimental data are gathered. Also a comparison will be made of the total acoustic power radiated by the interacting jet flows and that of the single jet flow at lower pressures where the normal shock disc does not appear. Power level data are not yet available for the main jet alone below 50 psig to make the comparison possible.

Main Jet with 45° Impingement

The variation of power level with percent impingement for the 45° impinging flow has been established for a range of x/D values. These data are presented in Fig. 11. The basic behavior is similar to the one observed for the 90° impingement case but is not as well pronounced. The nominal values of percent impingement corresponding to maximum and relative minimum power level are higher than in the case of 90° impingement. Spectra for the case of 45° impingement are yet to be completed.

Shadowgraphs of the main jet flow interacting with the 45° impinging jet flow indicate the same general behavior as the case with 90° impingement and therefore are not presented here.

Discussion

It is generally accepted that there are three major noise generating mechanisms acting in high speed jet flows of the type reported here. These are: a) convected turbulence in the mixing region, b) shock-turbulence interaction, and c) resonance phenomena. The last mechanism is responsible for strong discrete noise radiation or screech, and according to Lighthill (Ref. 8) has been sufficiently described by Powell (Ref. 6). By its nature, the occurrence of resonance is favored in cold jets rather than hot jets (Ref. 9) and its presence in the latter can be eliminated by nozzle modification (Ref. 10) making it a surmountable practical problem. In recent years experimetal and analytical research efforts on noise from high speed jet flows have been directed at understanding the relative contributions made by each of the remaining two mechanisms (a) and (b) to the total noise radiated over a wide range of operating conditions. By and large the problem of the relative contributions of mechanisms (a) and (b) over a wide range of operating conditions is still unresolved (see, for example Refs. 11, 12 and 13). In addition to the three noise generating mechanisms (a), (b) and (c) listed above, the impinging annular jet flow can be considered as a separate and additional noise source in the interacting jet flows discussed here. The variation of total acoustic power radiated by the interacting jets as a function of percent control, may be discussed in terms of relative contributions from each of these four acoustic sources. First let us consider the experimentally observed increase in the total noise radiated over the first 8% impingement (Fig. 5). Considering the available experimental evidence, the following are considered to be

the significant sources contributing to the increase of the total noise radiated: a) the noise from the impinging annular jet flow, b) the expected increased turbulence level due to the mixing of the interacting jet flows, c) the observed increase in size of the reflected shocks. On the other hand, d) possibility of a decrease in turbulence level due to attenuation of the high velocity gradients in the shear region of the main jet flow due to the impingement of the annular jet flow, and e) the observed decrease in extent of the normal shock disc would result in decreased acoustic power radiation with increasing percent impingement. Since from 0 to 8% impingement, the power radiated increases, the total noise contribution from contributing sources a) to c) must be dominant. It is unlikely that the impinging jet flow noise at these low values of percent impingement is contributing significantly to the power level. Also in the available experimental data, there is no definitive evidence to suggest the existence of noise contributions from resonant phenomena. Increased turbulence may be making a significant contribution. The length of the reflected shocks, Fig. 10a, increases with increasing percent impingement, and significantly, this increase peaks approximately at the value of percent impingement at which the total noise peak occurs (compare Fig. 10a with Fig. 5). This strongly suggest that the increase in acoustic power radiation between 0 and 8% impingement may be dominated by the interaction of the convected turbulence (which itself may also be increasing) with the growing oblique shocks.

From 8 to 18% impingement the size of the shock structure changes only slightly (see Fig. 10a), but shock spacing varies, and at 18%

impingement a repetitive shock pattern is established. Over this range of impingement values, factors contributing to an increase in power radiated might be a) the noise of the impinging annular jet, b) increased turbulence level due to mixing of the interacting jet flows, c) the possible presence of resonant phenomena. However, the power radiated in this range of impingement values is observed to decrease. A possible explanation may be as follows: The impinging jet flow penetrates sufficiently the main jet flow and possibly causes a decrease in the high velocity gradients normally present in the exhausting flow of a single free jet. This may result in a reduced contribution to the turbulence level of the interacted jet flow. Furthermore, as pointed out earlier, the normal shock disc is receding towards the main jet exit and the repetitive shock structure is progressively established with increasing percent impingement. This behavior suggests that the interacted combined jet flows behave as a single free jet flow operated at decreasing pressure ratio. As pointed out earlier, the impinging flow increases the boundary pressure in the interaction regions and yields lower effective pressure ratios. At 18% impingement, the shock structure is repetitive. Any resonance mechanism which might be acting under these operating conditions is blocked by the annular jet flow. This interruption of the feedback system by the annular jet in essence is similar in its effect to the technique used by Hammitt (Ref. 14), where he employed a sound deadening reflective baffle. Therefore from 8 to 18% impingement the inter-

acted jet flow is effectively acting as a single free jet operating at decreasing pressure ratios without the occurrence of resonant phenomena, thus resulting in a decrease of acoustic power radiation.

Between 18 and 50% impingement the power radiated increases. Above 18% impingement, annular eddies appear in the interacted jet flow (close to the shoulder of the reflected shocks in Figs. 9e and 9f). As evidenced by the extended reflected oblique shocks (Fig. 9e), the combined interacted jet flow is supersonic almost over its entire width. Close examination of the original photographs at high values of percent impingement, reveals a number of acoustic sources of strong discrete radiation (f = 28 kcps). This would indicate a possible resonance phenomenon occurring at the high values of percent impingement. This plus increased turbulence level and the contribution of the noise of the impinging jet flow, which has significant velocity at these conditions, may account for the increase in power radiation at the higher values of percent impingement.

The foregoing explanations of the observed behavior of the acoustic power radiation from interacting jet flows are of course tentative and further experimental and analytical work is planned to verify the reasoning.

Paper Presented

A paper reporting the salient features of the results presented here on the noise from high speed impinging jet flows was presented by the authors on June 3, 1966 at the 71st meeting of the Acoustical Society of America held in Boston. The abstract appeared in the meeting program. Following the completion of the present phase of the experimental work in progress and the analysis of the experimental data, by September 1966, a report will be submitted to NASA for publication.

Bibliography

1. Dosanjh, D. S. and Montegani, F. J., "Noise Investigations with Impinging Jet Flows," (Status Report No. 2), Report No. ME1085-64062, Syracuse University Research Institute, (1964).

2. Dosanjh, D. S. and Montegani, F. J., "Noise Investigations with Impinging Jet Flows," (Status Report No. 3), Report No. ME1085-64113, Syracuse University Research Institute, (1964).

3. Dosanjh, D. S. and Montegani, F. J., "Noise Investigations with Impinging Jet Flows," (Status Report No. 4), Report No. ME1085-65054, Syracuse University Research Institute, (1965).

4. Dosanjh, D. S. and Montegani, F. J., "Noise Investigations with Impinging Jet Flows," (Status Report No. 5), Report No. ME1085-651205, (1965), STAR N66-14633.

5. Lassiter, L. W. and Hubbard, H. H., "The Near Noise Field of Static Jets and Some Model Studies of Devices for Noise Reduction," NACA TN 3187, 1954.

6. Powell, A., "On the Mechanism of Choked Jet Noise," Proceedings Royal Society, B. Vol. 66, 1953.

7. Love, E. S., et at., "Experimental and Theoretical Studies of Axisymmetric Free Jets," NASA TR-R-6, 1959.

8. Lighthill, M. J., "On Sound Generated Aerodynamically," Part II, Proceedings Royal Society, A. Vol. 222, 1954.

9. Lee, R. and Smith, E., et al., "Second Biannual Progress Report Program of Research on Noise Suppression," Appl. Res. Operation, Flight Propulsion Laboratory, Department, General Electric Company, Evendale, Ohio, June, 1960.

10. Fowell, L. R. and Korbacher, G. K., "A Review of Aerodynamic Noise," UTIA Review No. 8, July, 1955.

11. Richards, E. J., "On the Noise from Supersonic Jets," J. Roy. Aeronaut. Soc., 61, 43-5, January 1957.

12. Westervelt, P. J., "Aerodynamic Noise: Its Generation and Suppression," General Eng. Lab., General Electric Report No. 57GL222, July 1957.

13. Howes, W. L., "Similarity of Far Noise Fields of Jets," NASA TR-R-52

14. Hammitt, A. G., "The Oscillation and Noise of an Overpressure Sonic Jet," General Applied Science Laboratories, Tech. Rept. No. 137, November 1959.

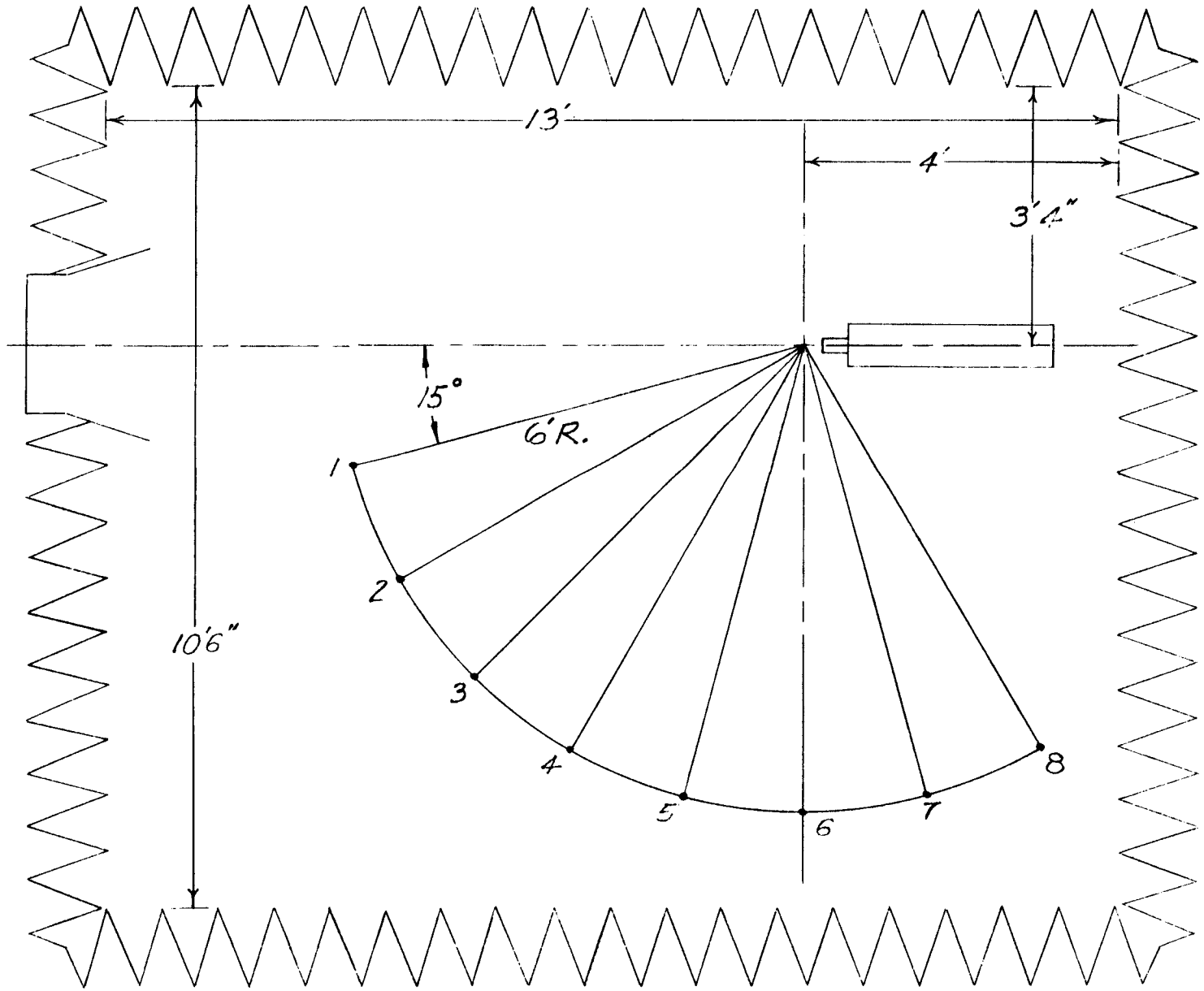

Fig. 1 Schematic arrangement of the jet nozzle location and the measuring stations in the anechoic chamber.

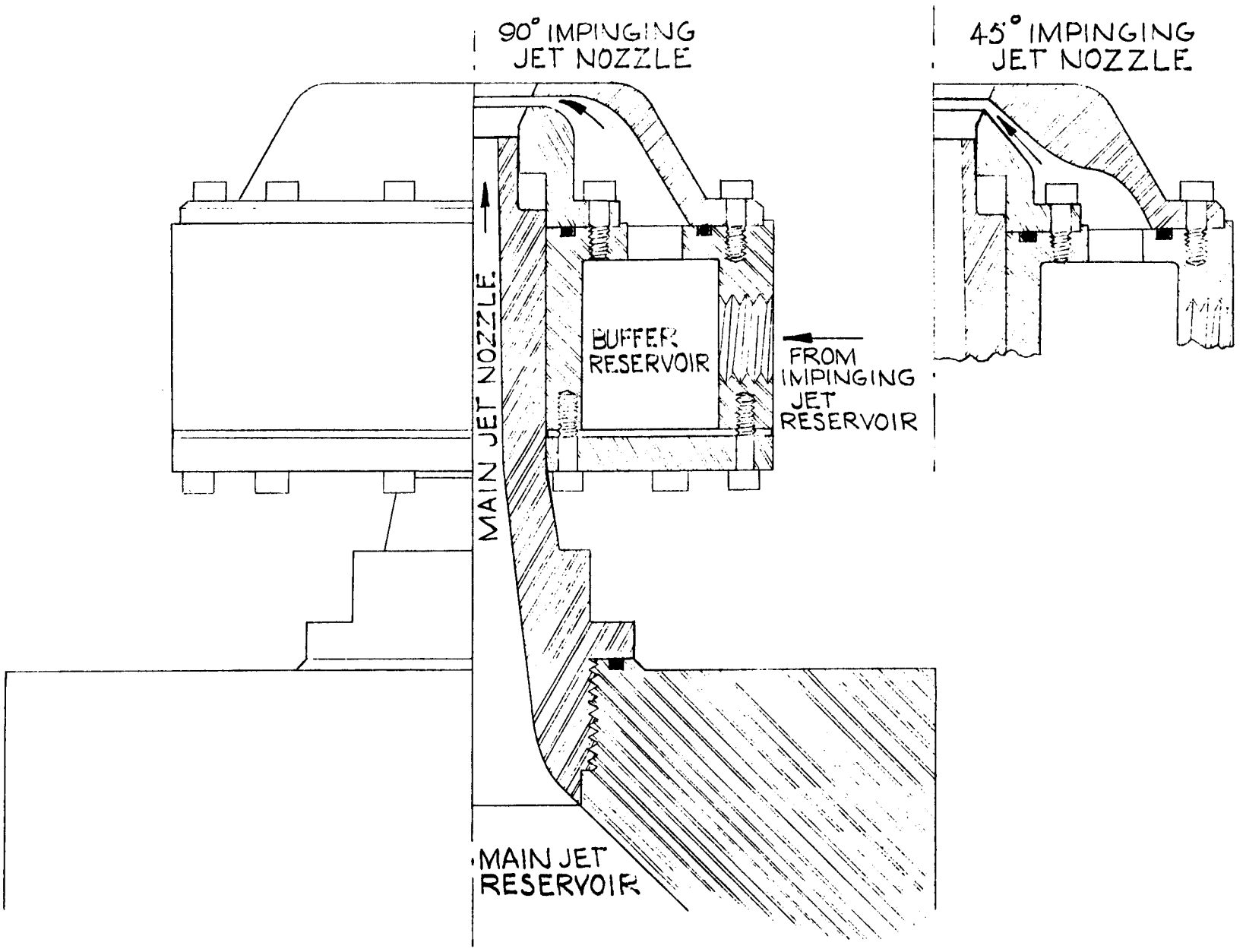

Fig. 2 Nozzle arrangement. Main jet diameter = 3/8 in. Impinging jet dimensions: 3/4 in. diam. x 3/64 in. wide.

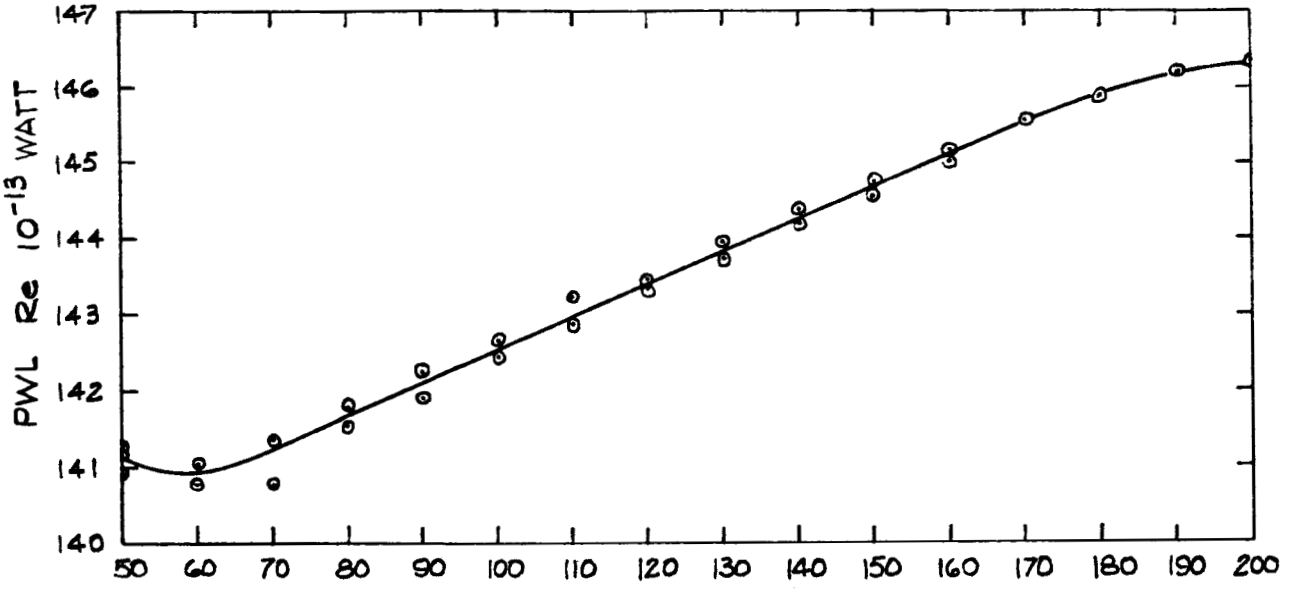

a) Total acoustic power radiated.

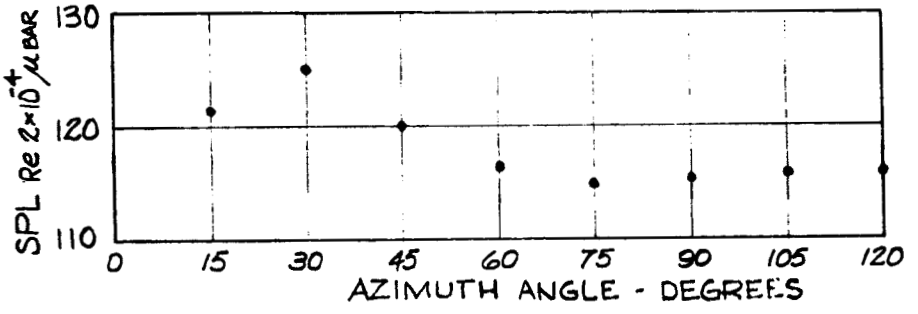

b) Overall sound pressure level versus direction at a radius of 192D.

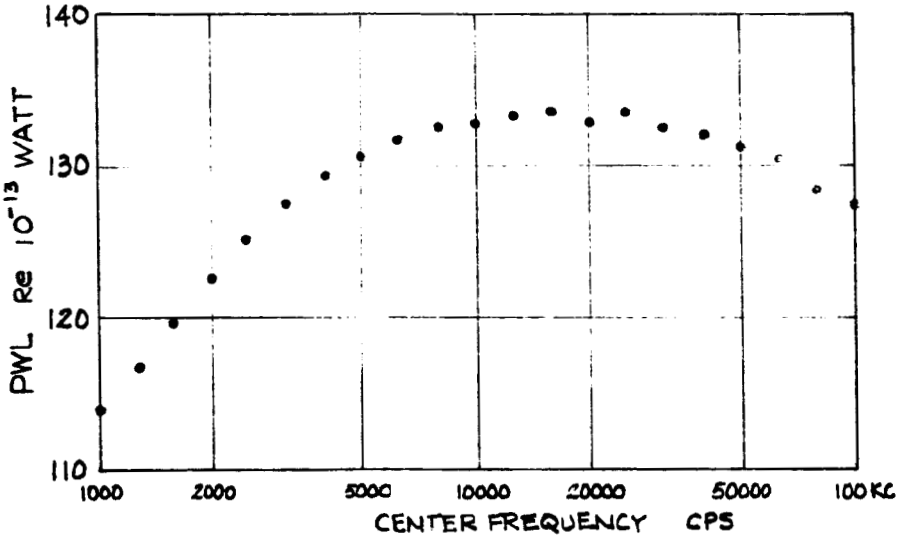

c) 1/3 octave band power spectrum.

Fig. 3 Acoustical data for 3/8 in. diam. main jet operated at 100 psig with impinging jet nozzle removed.

POP	POC	X/D	PJ	CJ	RADIUS	CHIMP	COMMENT
100.00	0.00-0.3333		1	0	72.00	41.22	NO CJ

SPECTRUM ANALYSIS

	THETA	15	30	45	60	75	90	105	120
NO.	FREQ.	SPL(F,THETA)							
12	315	82.0	0.0	0.0	0.0	0.0	0.0	0.0	0.0
13	400	85.5	81.0	0.0	0.0	0.0	0.0	0.0	0.0
14	500	89.8	85.0	0.0	0.0	0.0	0.0	0.0	0.0
15	630	91.5	88.4	81.3	0.0	0.0	0.0	0.0	0.0
16	800	95.3	91.8	84.4	80.3	0.0	0.0	0.0	0.0
17	1000	98.3	95.5	87.5	82.6	81.6	80.3	0.0	0.0
18	1250	101.4	98.8	91.2	85.3	84.3	82.6	81.0	0.0
19	1600	103.5	102.4	94.5	87.5	86.3	84.6	83.0	81.3
20	2000	105.4	105.6	97.6	90.0	88.5	86.7	85.3	83.9
21	2500	108.0	108.7	100.9	92.0	90.5	88.6	87.3	85.7
22	3150	108.3	111.0	103.7	94.2	92.2	90.5	88.9	87.9
23	4000	109.5	113.1	106.5	96.5	93.9	92.2	90.6	89.8
24	5000	110.4	114.0	108.2	98.0	94.4	93.4	92.1	91.1
25	6300	111.1	115.2	109.5	99.6	96.7	94.9	93.5	92.8
26	8000	112.3	115.5	109.7	101.0	98.2	96.1	95.0	96.3
27	10000	112.5	115.7	109.8	102.0	98.9	97.3	98.5	103.9
28	12500	112.4	114.8	109.0	102.5	99.5	99.8	105.8	107.5
29	16000	111.5	114.3	108.6	103.4	100.7	106.1	107.9	107.6
30	20000	109.8	113.3	108.2	103.6	103.7	107.0	106.3	105.9
31	25000	108.2	112.8	108.7	105.1	107.2	106.3	105.6	106.1
32	31500	106.2	111.2	108.4	107.1	106.2	104.9	106.1	106.0
33	40000	104.2	109.7	107.9	108.9	105.0	105.2	106.0	105.4
34	50000	101.8	108.5	106.8	107.8	104.3	105.1	105.3	104.4
35	63000	100.5	106.5	106.2	106.9	105.0	105.3	104.9	103.5
36	80000	97.8	103.9	103.9	104.5	103.4	103.5	103.0	101.3
37	100000	96.1	103.1	103.1	103.3	102.9	102.8	102.0	100.1

SPL COMPUTED FROM SPECTRUM DATA

THETA	15	30	45	60	75	90	105	120
SPL	121.68	124.97	119.97	116.41	114.75	115.24	115.76	115.75

TOTAL ACOUSTIC POWER RADIATED

PWL	WATTS
143.64	0.2313E 02

Fig. 4 Typical computer printout of sound data analysis for main jet operating at 100 psig with impinging jet nozzle removed.

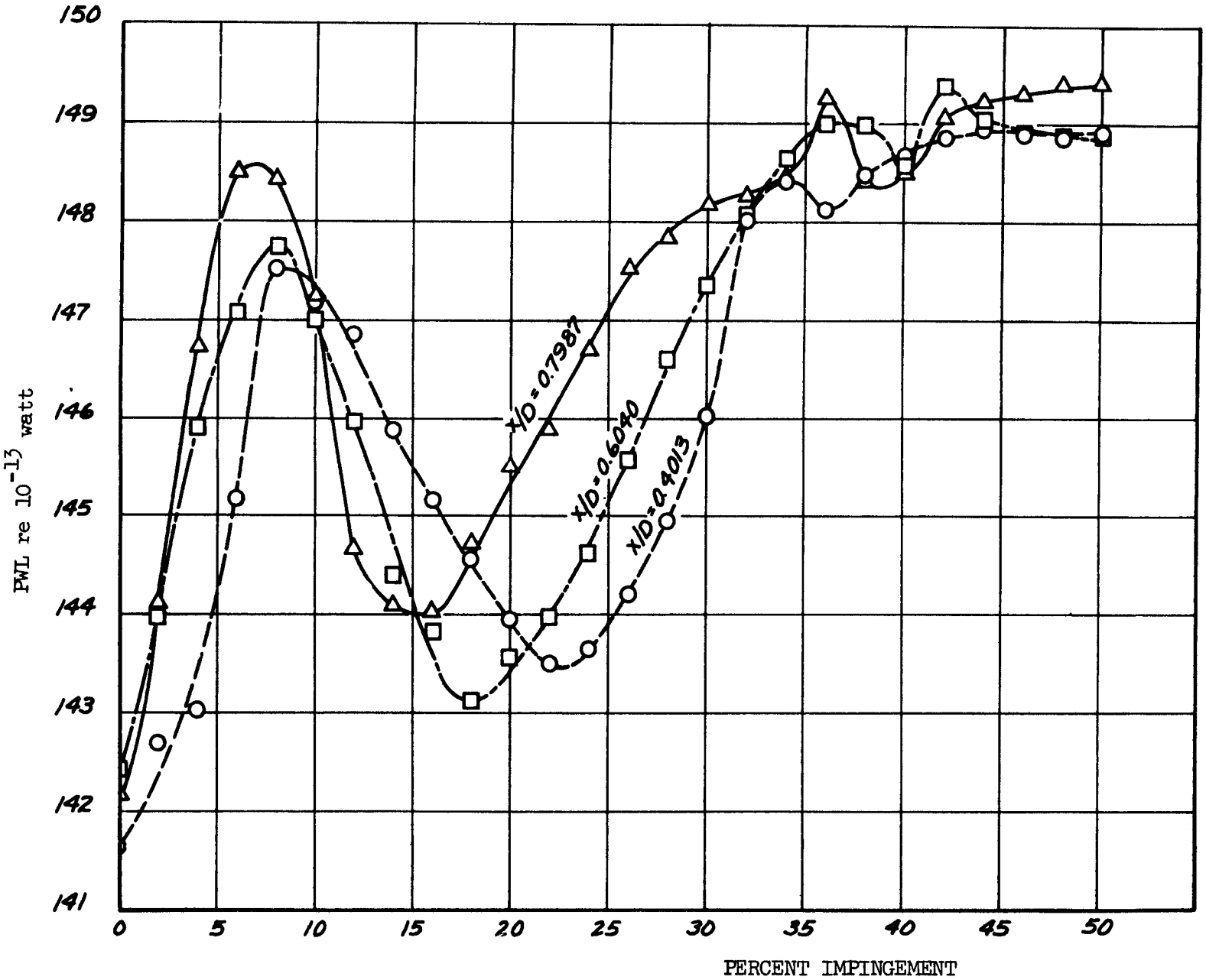

Fig. 5 Total acoustic power as a function of percent impingement. 90° interaction.

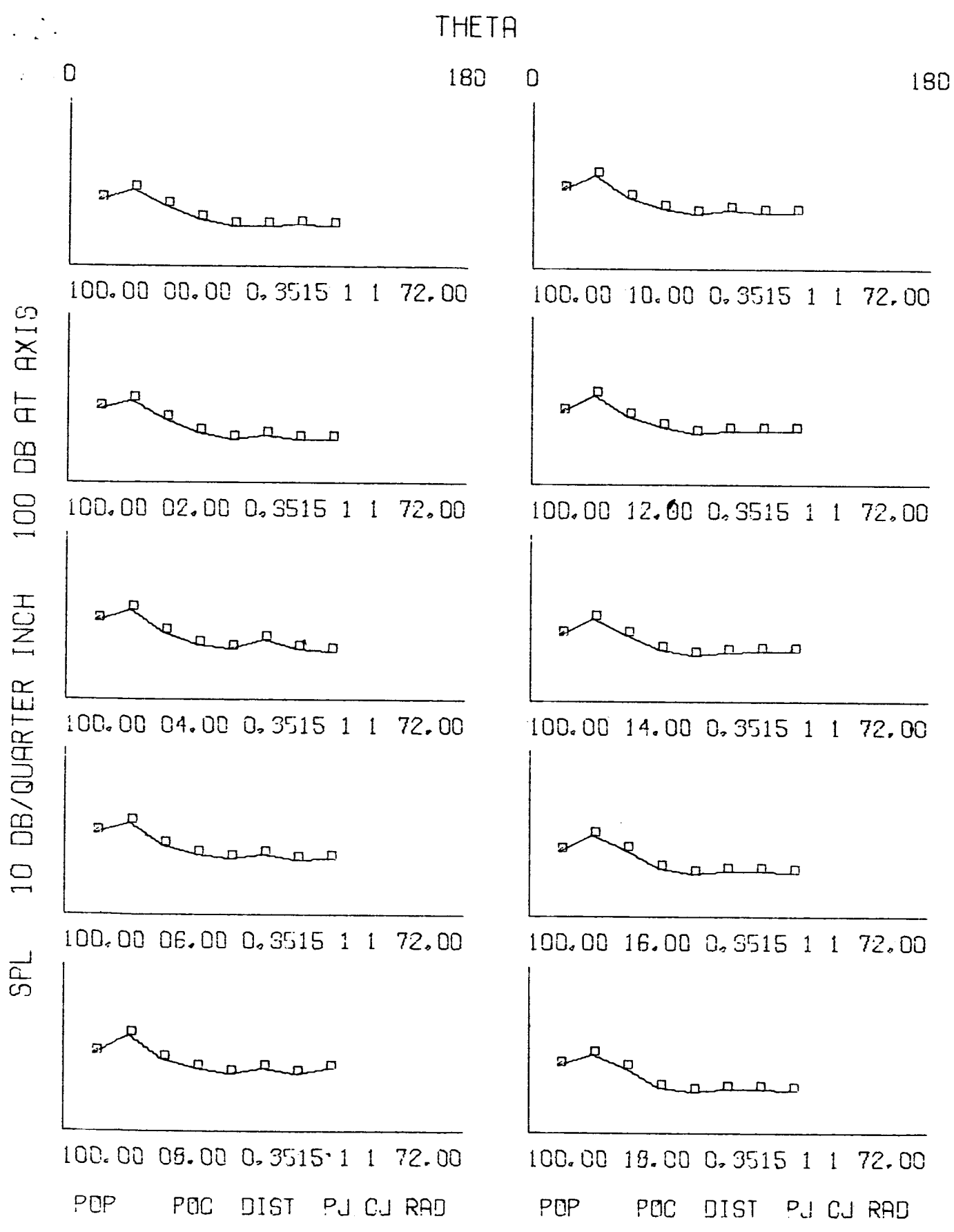

Fig. 6a Overall sound pressure levels versus direction at a radius of 192D for different values of percent impingement (POC). Impingement at 90° at x/D = 0.600.

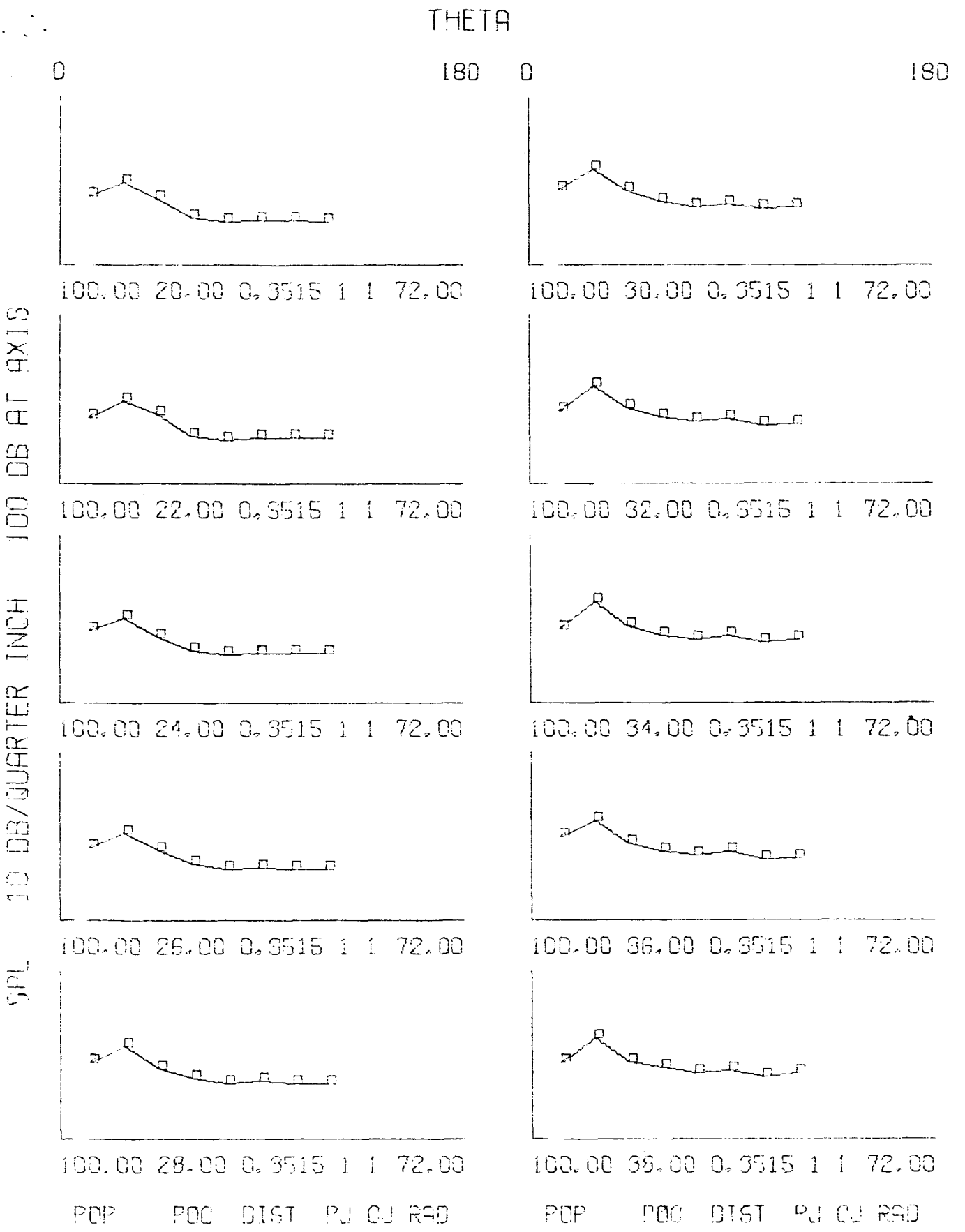

Fig. 6b Overall sound pressure levels versus direction at a radius of 192D for different values of percent impingement (POC). Impingement at 90° at x/D = 0.600.

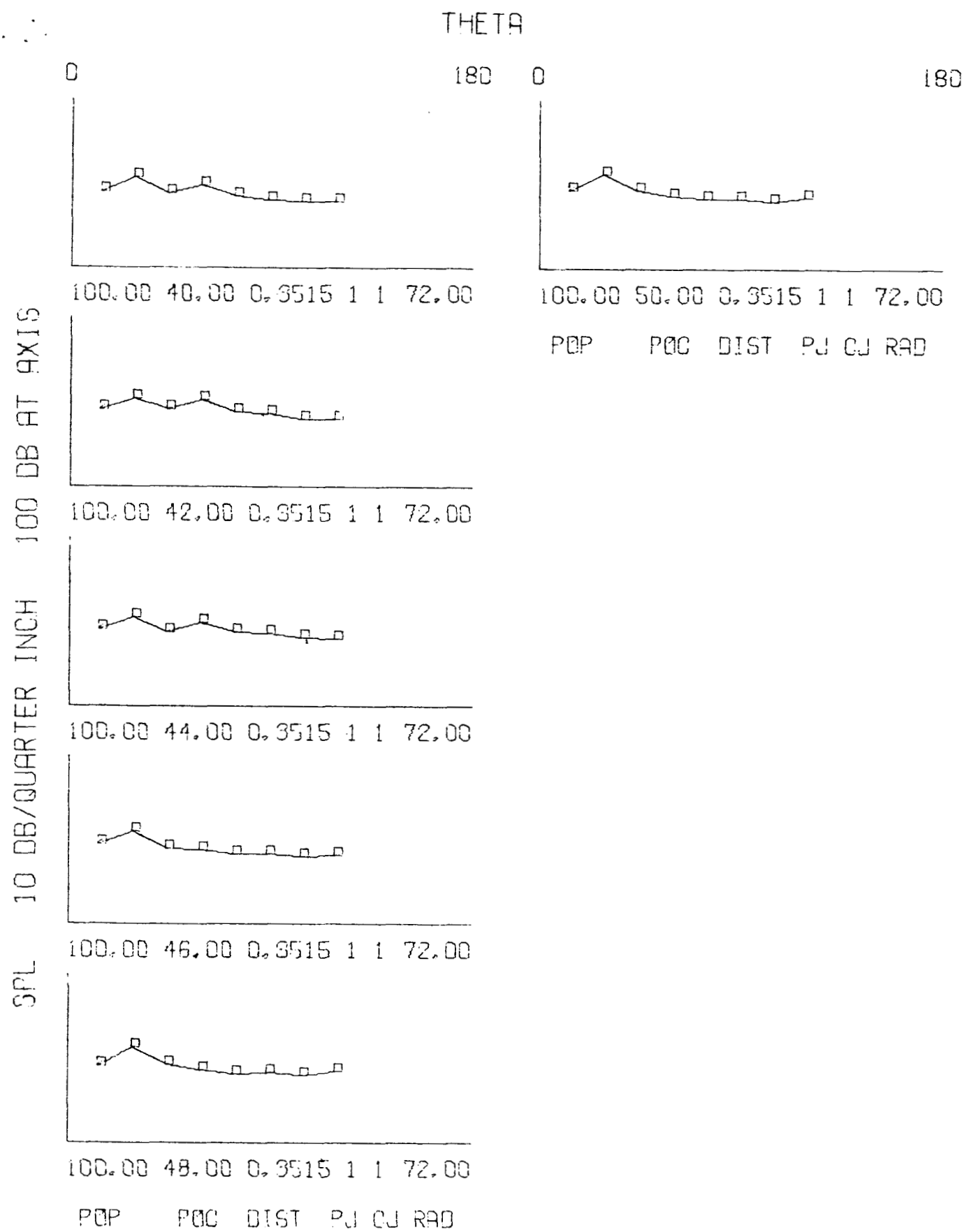

Fig. 6c Overall sound pressure levels versus direction at a radius of 192D for different values of percent impingement (POC). Impingement at 90° at x/D = 0.600.

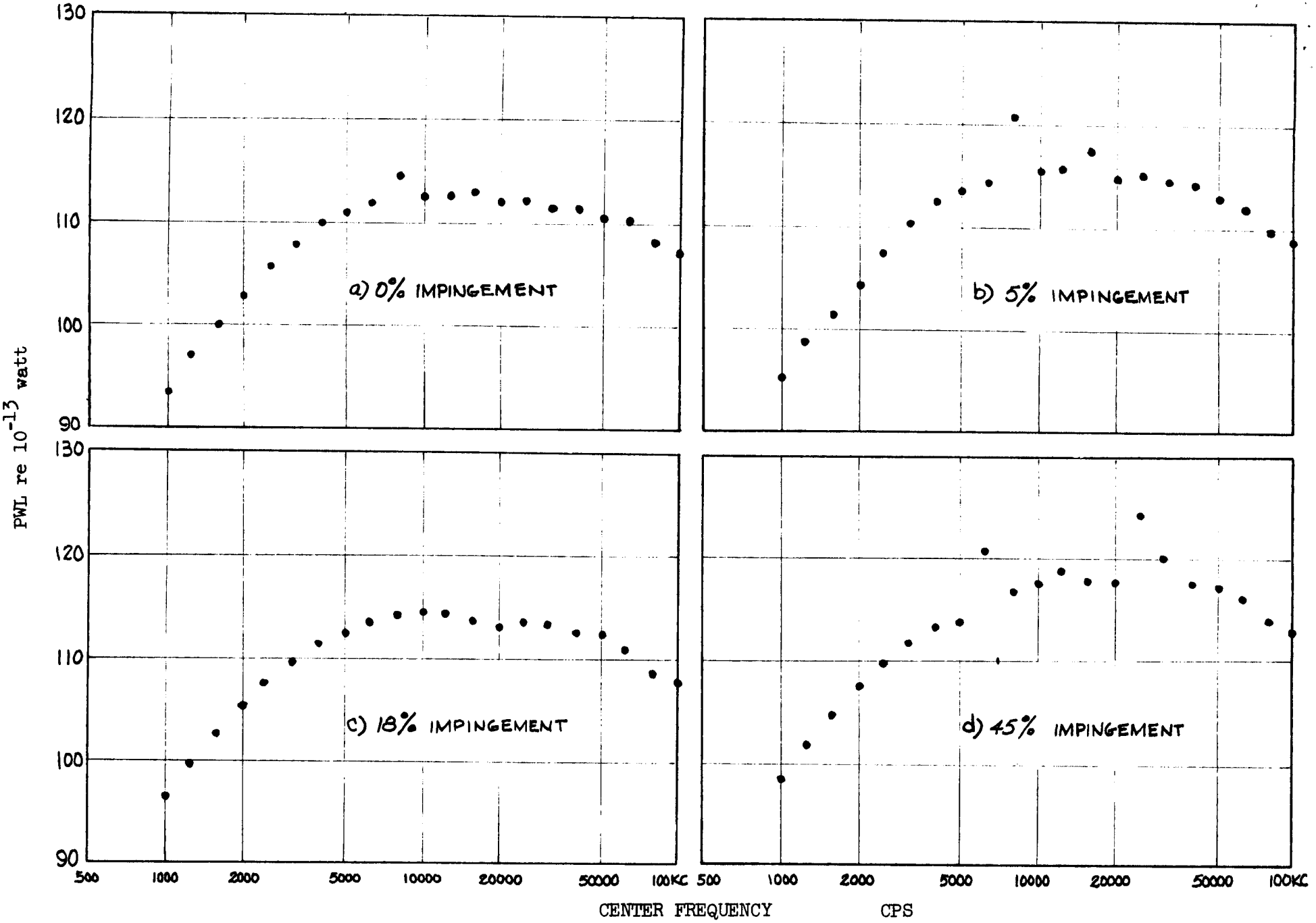

Fig. 7 1/3 octave band power spectra for 90° interaction at x/D = 0.600.

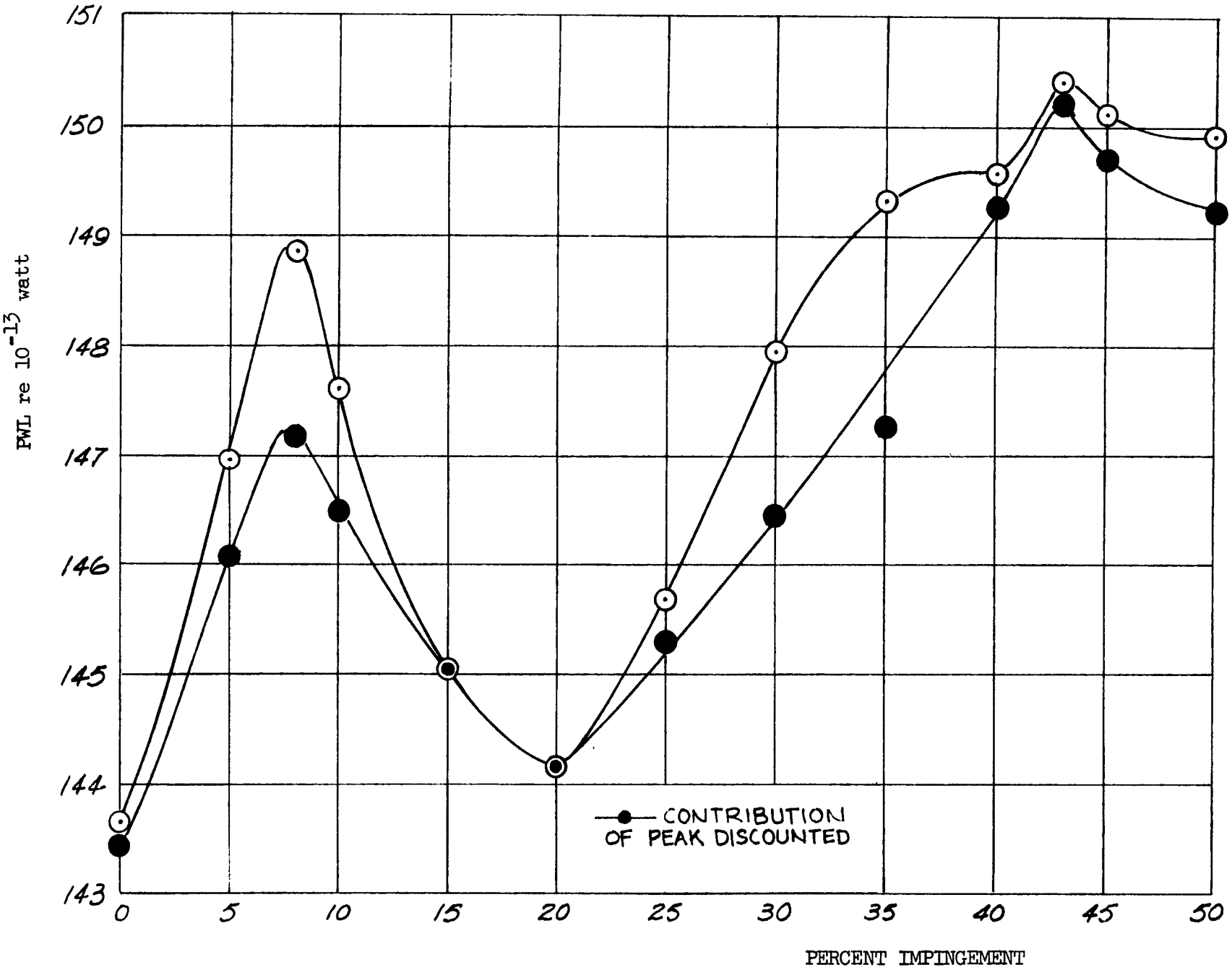

Fig. 8 Total acoustic power radiated by 90° interacting jets at x/D = 0.600.

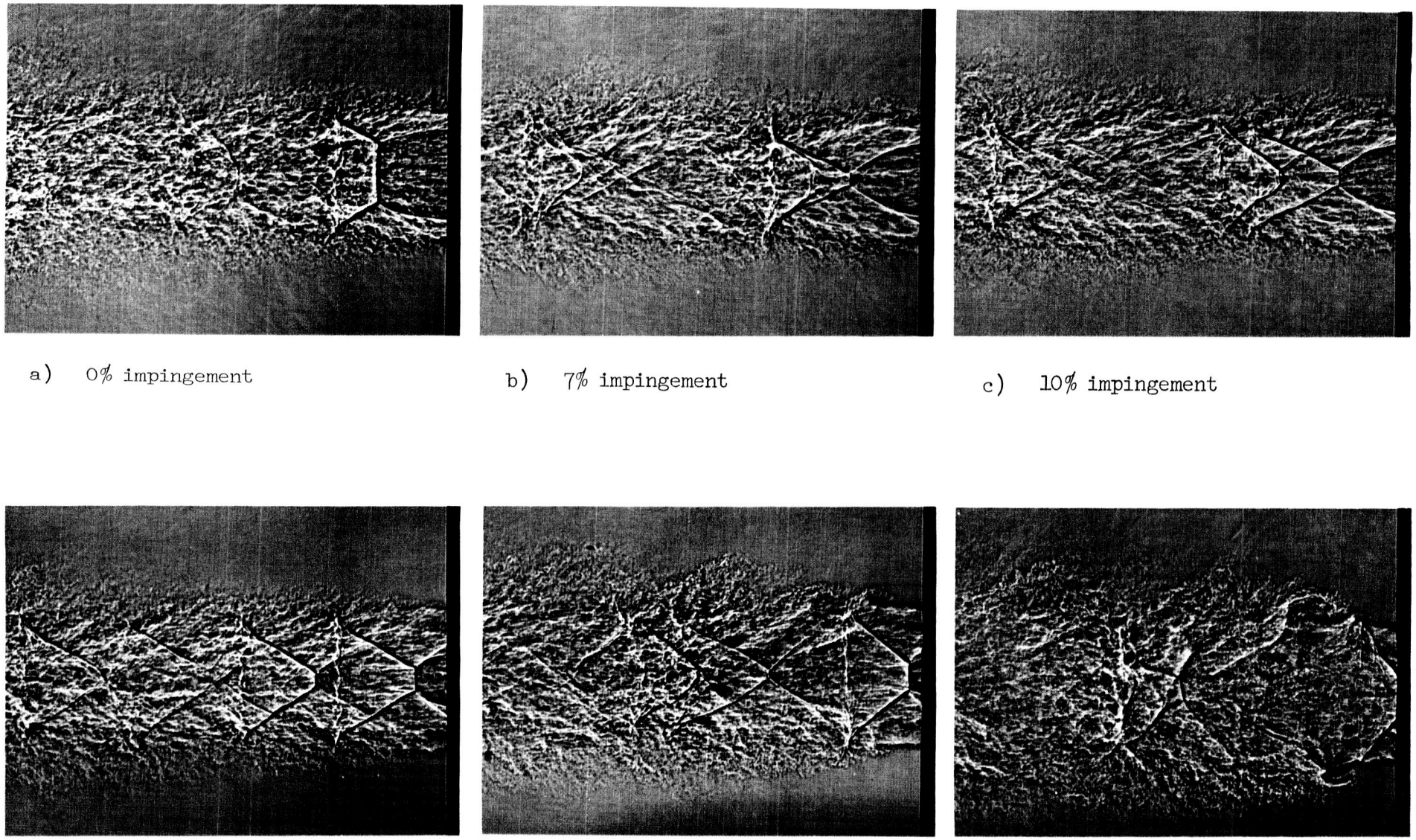

a) 0% impingement

b) 7% impingement

c) 10% impingement

d) 18% impingement

e) 30% impingement

f) 50% impingement

Fig. 9 Shadowgraphs of 90° interacting jets at x/D = 0.600.

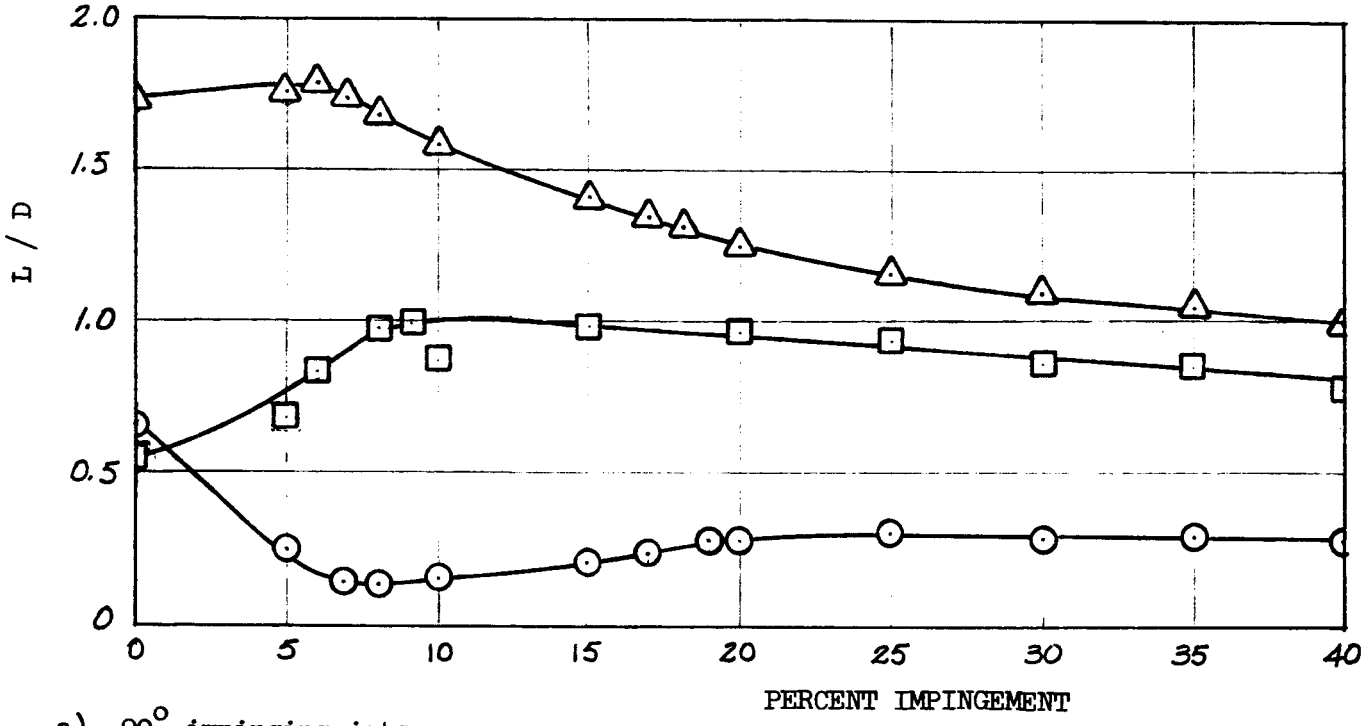

a) 90° impinging jets.

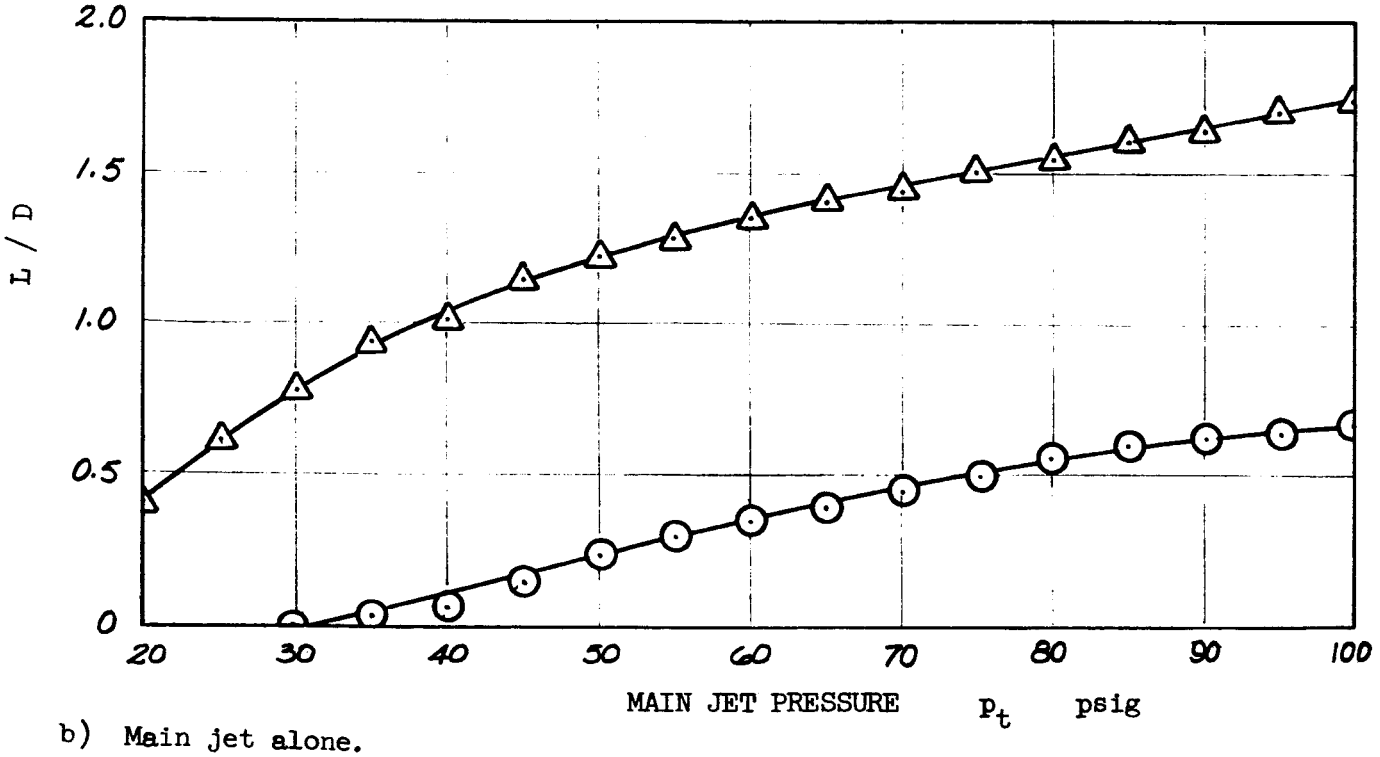

b) Main jet alone.

Fig. 10 Shock geometry. D = 3/8 in.

Cell length

Normal shock diameter

Reflected shock length

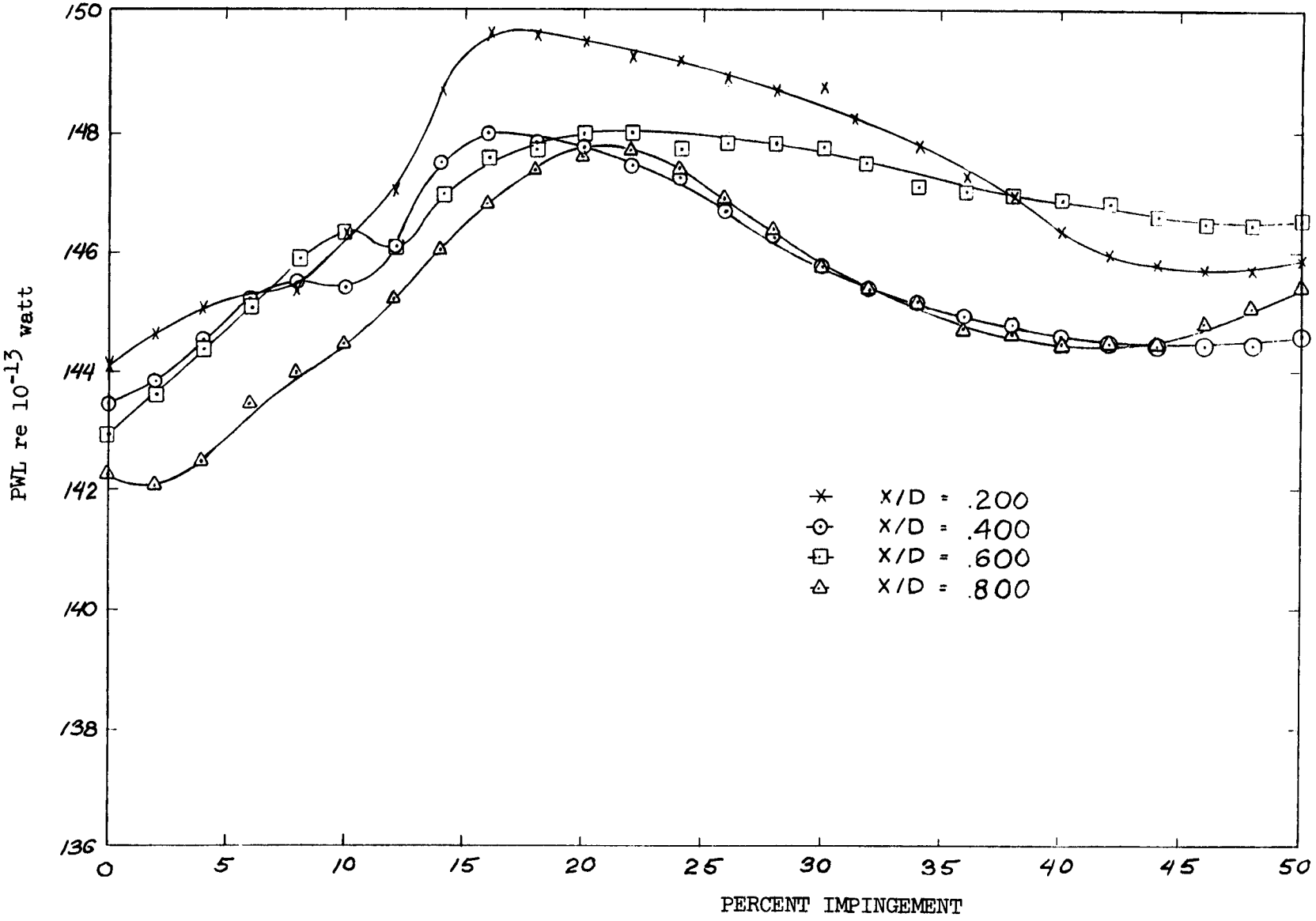

Fig. 11 Total acoustic power as a function of percent impingement. 45^{o} interaction.